

## Self-Diffusion of Poly(propylene imine) Dendrimers in Methanol

Ivo B. Rietveld\* and Dick Bedeaux

*Colloid and Interface Science Group, LIC, Gorlaeus Laboratories, Leiden University, P.O. Box 9502, 2300 RA Leiden, The Netherlands**Received March 21, 2000*

**ABSTRACT:** The self-diffusion coefficients have been determined for five generations of poly(propylene imine) dendrimers in methanol at three different temperatures—5, 25, and 45 °C—over the whole concentration range. Pulsed field gradient spin echo NMR has been used. The Stokes–Einstein hard sphere radii have been calculated in the zero concentration limit. They were equal, within error, to the radii found from the viscosity. The high-generation dendrimers have three concentration regimes: a dilute, a semidilute, and a concentrated regime. For the lower generations, only a dilute and a semidilute regime can be found. In the dilute regime, the self-diffusion coefficient decreases as a function of the concentration. In the semidilute regime, this decrease continues. In part of the semidilute and in the concentrated regime diffusion was very slow, and we were not able to measure the long time self-diffusion coefficient. As the transition from semidilute to concentrated solutions corresponds to a decrease of the radius of the dendrimer, dendrimers in concentrated solutions can be considered as collapsed though still separate molecules. The behavior in the semidilute and the concentrated regimes is very different from polymer diffusion.

## Introduction

Dendrimers are very regularly and precisely defined molecules. Nowadays they seem to become more and more popular for use in many different applications as catalysis, light harvesting, and drug targeting. With this growing interest for the use of dendrimers, knowledge about their physical properties becomes more important. Applying this knowledge can improve the efficiency of the dendrimers in their applications. Furthermore, the regularity and monodispersity of the dendrimers makes them very interesting model systems. They help to understand the behavior of highly branched polymers. Those polymers are often much less well-defined and therefore less suitable for a systematic study of their physical properties. In applications, however, they are cheaper in use since they are much easier synthesized. Moreover, they can form much larger structures than the average dendrimer, which can be an advantage in real applications.

The dilute solution properties of the dendrimers are thoroughly investigated. These studies were performed using neutron scattering,<sup>1,2</sup> viscosity,<sup>3</sup> gel permeation chromatography,<sup>4</sup> mass spectrometry,<sup>5</sup> computer simulations,<sup>6,7</sup> and methods that are more application based.<sup>8</sup> A picture of the structure and behavior of dendrimers evolves gradually from their results. As understood now, dendrimers have a dense core with back-folding branches.<sup>6,9</sup> The density has a maximum in the center. Usually a density plateau is found that, depending on the choice of dendrimer and experiment, falls off fast or slow to a low density tail.<sup>2,6,9–14</sup> Moreover, in dilute solutions these approximately spherical molecules behave like hard spheres. Swelling of dendrimers in simple solvents seems to be present but is much less than for normal polymers.<sup>6,14–16</sup>

To our knowledge, the diffusion properties of dendrimers have not yet been studied thoroughly. Only a few studies, to determine the diffusion coefficient in the zero concentration limit and the resulting hard sphere radii<sup>17,18</sup> and the influence of the pH,<sup>19,20</sup> have been published. Furthermore, only a few experimental papers

have been published about properties of concentrated solutions using viscometry<sup>3,21</sup> or neutron scattering.<sup>21–23</sup> In an earlier paper<sup>22</sup> we found, from the inverse osmotic compressibility, that dendrimers have three concentration regimes. First, the dilute regime where all dendrimers are separate spheres. The dilute regime can be subdivided into a very dilute regime, where the dendrimers behave like hard spheres and a denser regime,  $\phi > 0.18$ , where the solvation layers overlap. Second, at about 0.3 volume fraction, the beginning of the semidilute regime, the distance between the centers of the dendrimers becomes equal to twice the radius of gyration, causing them to shrink with increasing concentration. This is confirmed by a small-angle neutron scattering paper by Topp et al.<sup>23</sup> In semidilute solutions, dendrimers form a close-packed system of soft spheres, with little interpenetration and no network formation.<sup>3</sup> Finally, at very high concentrations the 5th and 4th generations are found to resist any further shrinking. This is then called the concentrated regime.

In this paper self-diffusion of dendrimers in dilute, semidilute, and concentrated solutions is studied. The self-diffusion coefficient is measured using field gradient NMR. Self-diffusion measurements make it possible to study the motion of separate dendrimers in solution. The self-diffusion coefficient can be found for a short time limit and a long time limit.<sup>3</sup> In the long time limit, the particle is slowed down due to correlations with other particles. Therefore, the long time diffusion coefficient is smaller than the short time diffusion coefficient. In a very dilute solution limit, the short and long time self-diffusion coefficients become equal. This limiting value is called  $D_0$ .

For  $D_0$ , the diffusion is entirely dependent on the size of the particle and the solvent. For a spherical particle we use the Stokes–Einstein equation

$$D_0 = \frac{k_B T}{6\pi\eta r} \quad (1)$$

where  $k_B$  is Boltzmann's constant,  $T$  the absolute temperature,  $\eta$  the viscosity of the solvent, and  $r$  the

effective hydrodynamic radius. This hydrodynamic radius of the sphere can therefore be determined by measuring the low concentration diffusion coefficient.

For a finite volume fraction ( $\phi$ ), the virial expansion can be used for the self-diffusion ( $D_s$ ) in dilute solutions:

$$D_s(\phi) = D_0(1 + k\phi) \quad (2)$$

Here the slope  $k$  may depend on temperature. The volume fraction is calculated from the ratio of the specific weights times the weight fraction.

With pulsed field gradient stimulated echo (PFGSE) NMR, the diffusion coefficient can be determined using the following relation for the amplitude of the Fourier transform of the acquired signal,  $A_G$ :<sup>24</sup>

$$A_G = A_0 \exp\left(-\gamma^2 G^2 \delta^2 D\left(\Delta - \frac{\delta}{3}\right)\right) \quad (3)$$

with  $A_0$  the echo amplitude at zero magnetic field gradient,  $\gamma$  the gyromagnetic ratio of the nucleus,  $G$  the gradient amplitude,  $\delta$  the length of the gradient pulse,  $\Delta$  the gradient pulse interval, and  $D$  the self-diffusion coefficient of the monitored nuclei.

In this paper the diffusion behavior is presented of the poly(propylene imine) dendrimer in methanol for the entire range of concentrations, dilute solution to pure substance. This has been measured for three different temperatures, 5, 25, and 45 °C. The hydrodynamic radius is found from the diffusion coefficient in the zero concentration limit. The different diffusion regimes are discussed.

## Materials and Methods

The poly(propylene imine) dendrimers were purchased from DSM (Geleen, The Netherlands) in different generations ranging from 1 up to 5. The following specifications were given by the producer: a water content varying from 4.5 down to <0.1 wt %, a toluene content of <0.1 wt % and containing cobalt up to at most <8 ppm. Methanol p.a. was purchased from Baker and used without further purification.

The samples were prepared as follows. All generations were dried for 3 days under vacuum at 40 °C to remove as much solvents as possible. They were subsequently dissolved in methanol and measured. The concentrations ranged from 1 up to 100 wt %. Concentrations were determined by weighing. Sample preparation was performed under a nitrogen atmosphere to keep the water content as low as possible.

The self-diffusion measurements were performed with the pulsed field gradient NMR method.<sup>25</sup> A Bruker AM200 has been used with a wide bore magnet of 4.7 T. It was connected to a Bruker Aspect 3000 spectrometer. A magnetic field gradient,  $G = 4.3 \text{ T m}^{-1}$ , was generated at a maximum current of 12 A by an actively shielded gradient coil, constructed at Massey University, Palmerston North in New Zealand, by the group of Prof. P. T. Callaghan. A Techon 7570 amplifier, coupled to the spectrometer, delivered almost rectangular gradients of a duration of 20 ms. Radio-frequency (rf) pulses were chosen in such a way that the magnetization changed 90° from the  $z$  axis in the  $x$ - $y$  plane (and back) at about 7  $\mu\text{s}$ . Different diffusion times were used to check for any time dependence in the measured diffusion. After each gradient pulse was a delay of 1.2 ms, to allow for the relaxation of possible eddy current, before the application of the rf pulse or the signal accumulation. The pulsed field gradient stimulated echo method<sup>26</sup> has been used, because the longitudinal relaxation time ( $T_2$ ) of the dendrimers was larger than the transversal relaxation time ( $T_1$ ). The experiments have been performed at three different temperatures, 5, 25, and 45 °C.

## Results

$D_0$  was determined by linear extrapolation of the low-concentration self-diffusion coefficients (cf. Figure 1) and

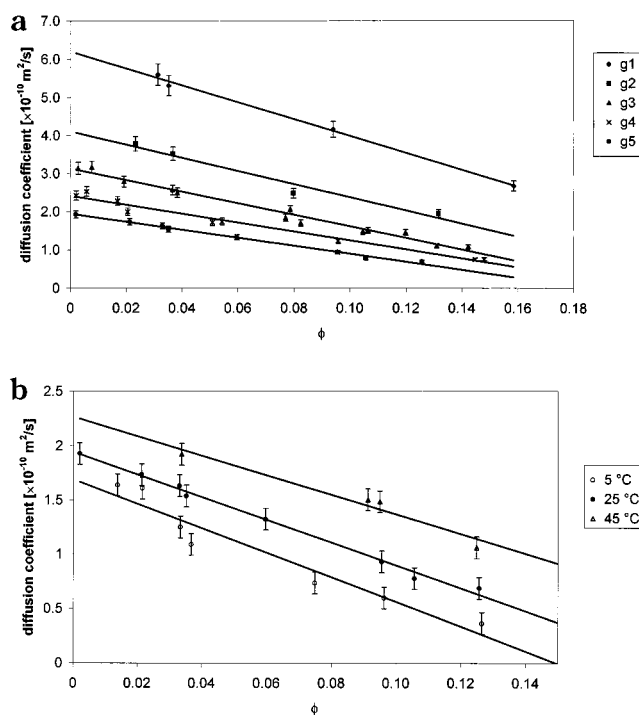


**Figure 1.** (a) Extrapolation of the low concentration diffusion coefficients for generations 1–5 to obtain  $D_0$  at 25 °C. (b) Diffusion of generation 5 for 5, 25, and 45 °C. The concentration is the thermodynamic volume fraction calculated from the specific volume. Errors (if not indicated) are of the same size as the markers.

**Table 1. Diffusion Coefficient [ $\times 10^{-10} \text{ m}^2 \text{ s}^{-1}$ ] at Zero Concentration for Five Generations at 5, 25, and 45 °C**

generation	5 °C	25 °C	45 °C
1	$4.3 \pm 0.3$	$6.23 \pm 0.10$	$7.4 \pm 0.2$
2	$2.8 \pm 0.2$	$4.36 \pm 0.05$	$5.0 \pm 0.1$
3	$2.22 \pm 0.09$	$3.15 \pm 0.06$	$4.1 \pm 0.2$
4	$2.11 \pm 0.02$	$2.42 \pm 0.06$	$3.4 \pm 0.1$
5	$1.70 \pm 0.12$	$1.97 \pm 0.02$	$2.28 \pm 0.13$

are given in Table 1. It is found that  $D_s$  follows a linear dependence up to a volume fraction of about 0.15. With increasing generation,  $D_s$  decreases in this domain. The negative slopes of lower generations are slightly steeper (cf. Figure 1a). The extrapolation for generation 5 for different temperatures is shown in Figure 1b.

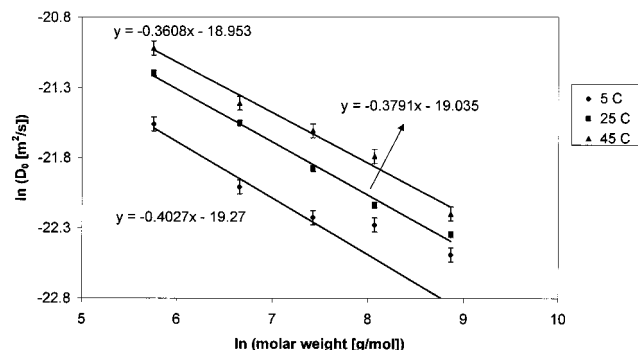
The hydrodynamic radii were determined using the Stokes–Einstein relation and given in Table 2. Tabulated temperature-dependent viscosities were used. Comparing the radii of 25 °C with radii from viscosity data at the same temperature,<sup>27</sup> we find that the values are within experimental accuracy the same. The radius of gyration ( $R_G$ ) is clearly smaller.<sup>1</sup> This indicates nondraining hard sphere behavior for all generations as was also concluded in an earlier paper.<sup>27</sup> The radius of gyration was determined from molecular dynamics (MD) calculations for a good solvent.<sup>1</sup> Experimental determinations in methanol and water show values slightly smaller than the MD results.<sup>22,28</sup>

Comparing the hydrodynamic radii for different temperatures, we find values that are independent of temperature for the lowest three generations within the experimental accuracy. For the 4th and more in particular for the 5th generation, the experiments show an increase with the temperature. In calculating the hydrodynamic volume fraction ( $\phi_H$ ), we shall use the radii from 25 °C for all temperatures and for all generations.

**Table 2. Radii [nm] from  $D_0$  Obtained Using Stokes–Einstein for Five Generations at Three Different Temperatures<sup>a</sup>**

generation	5 °C	25 °C	45 °C	$R_{\text{therm}}$ (ref 27)	$R_{\eta}$ (25 °C) (ref 27)	$R_G$ , good solvent (ref 1)
1	0.64 ± 0.04	0.64 ± 0.01	0.73 ± 0.02	0.50	0.65	0.50
2	1.00 ± 0.06	0.92 ± 0.01	1.08 ± 0.03	0.67	0.92	0.76
3	1.25 ± 0.05	1.27 ± 0.02	1.32 ± 0.05	0.86	1.21	1.01
4	1.31 ± 0.02	1.65 ± 0.04	1.58 ± 0.06	1.08	1.54	1.29
5	1.63 ± 0.11	2.03 ± 0.02	2.38 ± 0.14	1.37	1.98	1.59

<sup>a</sup> The radius obtained from the specific volume ( $R_{\text{therm}}$ ) is given, as well as the viscosity radius at 25 °C and the radius of gyration in a good solvent.

**Figure 2.** Scaling of  $D_0$  with the molar weight.

For the 4th and 5th generations at 5 °C the hydrodynamic radius is found to be equal to the radius of gyration. As explanation of this, we tentatively suggest the fact that methanol is a less good solvent for 5 °C, which causes the dendrimers to shrink. A molecular dynamics study shows the same influence of the solvent quality.<sup>29</sup> For generations higher than the fourth generation, they find a similar temperature dependence of the radius of gyration. Measurements of the second virial coefficient of the osmotic pressure of this dendrimer at 25 and 45 °C, on the other hand, did not show any convincing temperature dependence for the third and fifth generation.<sup>27</sup> In addition, a neutron scattering study does not show a convincing change of the radius of gyration on temperature for the higher generations of the PAMAM dendrimer.<sup>15</sup>

The scaling behavior of  $D_0$  with the molar weight gives a qualitative idea of the density distribution in the different generations of dendrimer. A scaling exponent of 0.5 reflects a fractal structure, 0.6 reflects a random coil polymer in a good solvent, 0.33 is for an object with a uniform density distribution, and 0.2 means a density increasing with the radius. The last option has been proposed by de Gennes.<sup>30</sup> Compared to the uniform density, the proposal of de Gennes leads to a larger radius. Computer simulations indicate a decreasing density distribution toward the outside<sup>9,12</sup> or a uniform density distribution.<sup>6,11,13</sup> Neutron scattering experiments indicate a maximum density in the core with a decreasing density toward the outside.<sup>2,10</sup> In Figure 2, the log of  $D_0$  is shown versus the log of the molar weight. At 25 and 45 °C, the exponents are found to be  $-0.38$  and  $-0.36$ . This implies a rather uniform density distribution. The somewhat higher value than 0.33 agrees with the presence of a decreasing density at the outer side of the sphere. For 5 °C, roughly the same slope is obtained for the first three generations. Given the slope, the molecules have a uniform density and do not have the de Gennes structure. The transition of the 4th and 5th generation at 5 °C is to a larger  $D_0$  and therefore to a smaller radius. The transition is therefore not to a de Gennes structure, which would

**Table 3. Initial Slopes  $k_H$  of the Diffusion Coefficient Dependence on the Hydrodynamic Volume Fraction  $\phi_H$ <sup>\*</sup>**

generation	5 °C	25 °C	45 °C
1	$-1.3 \pm 0.2$	$-1.6 \pm 0.1$	$-1.1 \pm 0.1$
2	$-1.3 \pm 0.2$	$-1.3 \pm 0.1$	$-1.1 \pm 0.1$
3	$-1.5 \pm 0.2$	$-1.5 \pm 0.1$	$-1.3 \pm 0.2$
4	$-1.7 \pm 0.1$	$-1.3 \pm 0.1$	$-1.4 \pm 0.2$
5	$-2.6 \pm 0.5$	$-1.7 \pm 0.1$	$-1.2 \pm 0.2$

<sup>a</sup> The volume is determined with the radius of 25 °C from Table 2.

have a larger radius, but to a more compact structure. This indicates that methanol at 5 °C is a less good solvent. We conclude that the molar weight dependence substantiates the view that the density distribution is uniform with a decreasing density at the outer side.

At 25 °C the hydrodynamic radius is found to grow linearly with the generation number. The relation  $R_H = 0.35 \times G + 0.25$ , with  $R_H$  the hydrodynamic radius in nanometers and  $G$  the generation, can be obtained. The exponentially growing molar weight with the generation number in combination with the linear growth of the hydrodynamic radius implies a minimum in the density of the dendrimer around generation 4 or 5. This causes the maximum in the specific viscosity as has already been thoroughly discussed.<sup>7,27,31–34</sup>

From the foregoing and from ref 27, it is clear that dendrimers in dilute solution behave as larger effective spheres than their specific volume accounts for. The radius of gyration is smaller than the hydrodynamic radius. Therefore, if the hydrodynamic interaction between the dendrimers is studied with eq 2, we use the hydrodynamic radius as the most suitable parameter to determine the volume fraction. Here we take the hydrodynamic radii from 25 °C, so that a possible temperature dependence of the radius remains visible in the virial coefficients. In Table 3 the resulting virial coefficients  $k_H$  are given.

For hard sphere hydrodynamic interaction in the case of long time self-diffusion, different values for  $k$  can be found in the literature. One of the most recent publications of Dhont gives  $k = -2.1$  for hard sphere behavior.<sup>35</sup> Other values in the literature are  $-2.68$  by Batchelor<sup>36</sup> and  $-1.89$  by Felderhof.<sup>37,38</sup> Although there is no agreement in the literature, hard sphere behavior is characterized by a larger absolute value of  $k$  than most values we find for  $k_H$ . If one uses the radius of gyration, rather than the hydrodynamic radius, to determine the volume fractions, the values range from  $-2.3$  to  $-3.5$  and are therefore usually larger in absolute values than the hard sphere values. We conclude that the dendrimers are soft spheres with an effective hard sphere radius, which is now determined from the virial coefficient, between the hydrodynamic radius and the radius of gyration. Only for the 4th and 5th generations for 5 °C are the hydrodynamic radius and the radius of gyration



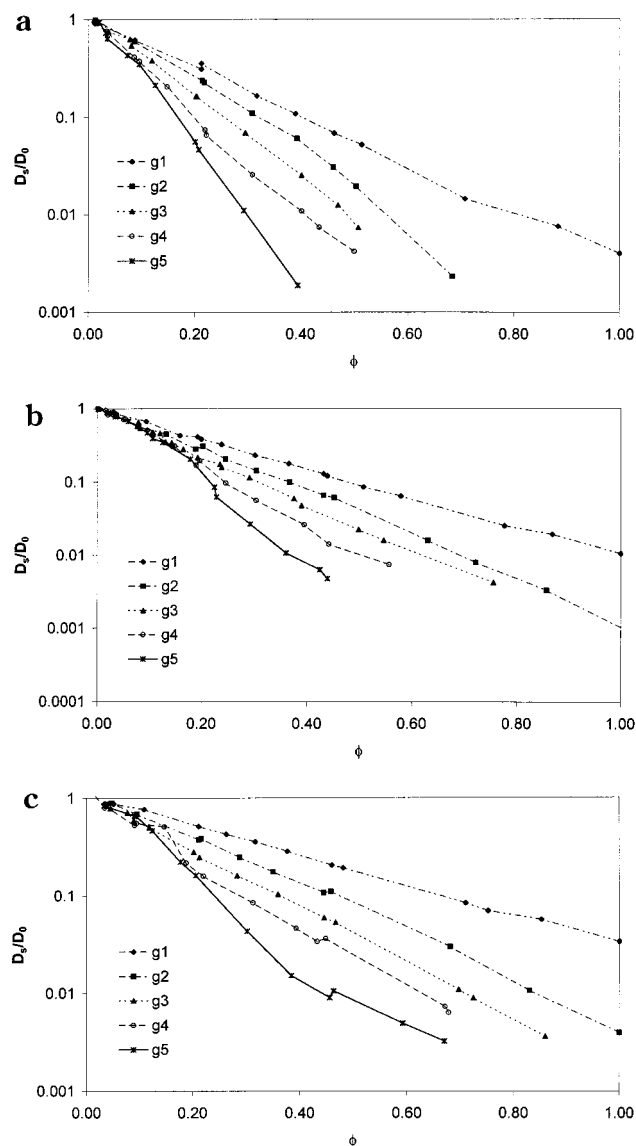


**Figure 3.** Overview of the behavior of the diffusion coefficients for the complete concentration range measured at (a) 5 °C, (b) 25 °C, and (c) 45 °C. The values are divided by  $D_0$  as given in Table 1. The concentration is expressed in thermodynamic volume fraction.

the same. In that case the dendrimers do not behave like soft spheres.

For volume fractions larger than 0.2 the virial expansion for the self-diffusion coefficient is no longer adequate. At this volume fraction the solvation layers start to touch each other. Many sphere hydrodynamic interactions become important. The calculation of higher order virial coefficients shows that positive contributions should be added to the linear decrease so that the diffusion coefficient remains finite.

In Figure 3a–c the diffusion coefficients divided by  $D_0$  from Table 1 are plotted logarithmically for the complete concentration range and for different temperatures. Generally, a decrease of the diffusion coefficient for all generations can be observed. Because of very small spin relaxation times,  $T_2$  and  $T_1$ , the diffusion coefficient could not be measured for higher volume fractions of generations 2, 3, and 4. This especially for 5 °C. It is clear from Figure 3 that, with the exception of the first generation, single-exponential behavior is not adequate to describe the diffusion behavior.

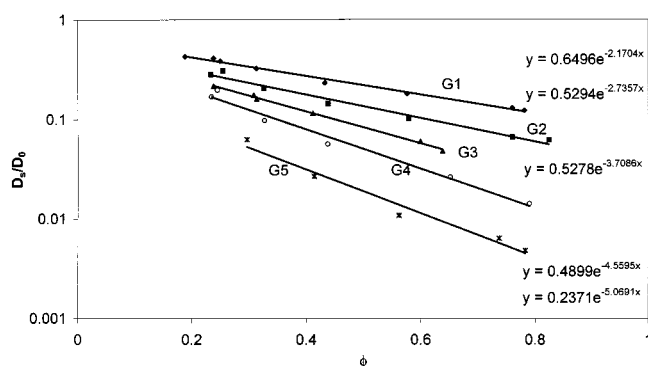


**Figure 4.** Semidilute regime. Application of the free volume theory (eq 4). The concentration is  $\phi/(1 - \phi)$ . The exponents are the  $\gamma$  values for overlap.

An alternative expression, to describe the diffusion behavior as a function of concentration, is given by the free volume theory, introduced by Cohen and Turnbull.<sup>39</sup> This theory was extended to self-diffusion in polymer solutions among others by Vrentas and Duda.<sup>40,41</sup> Callaghan used it in the following simple manner:<sup>42</sup>

$$D_s = D_0 \exp(-\gamma\phi/(1 - \phi)) \quad (4)$$

$D_0$  is a constant,  $\phi$  is the volume fraction taken by polymer, and  $1 - \phi$  is the “free volume” taken by the solvent.  $\gamma$  is an overlap factor. It is introduced, since the free volume is available to more than one polymer or dendrimer.

Plotting the diffusion coefficients versus  $\phi/(1 - \phi)$  should give a single-exponential curve, if the free volume theory applies. However, different fits for the low-concentration 0–0.2 volume fraction and 0.2–0.4 volume fraction are obtained. For the dilute regime eq 4 is equivalent to eq 2, one has  $\gamma = -k$ , and this has already been discussed. Between the volume fractions 0.2 and 0.4, the semidilute range, reasonable fits can be obtained. The resulting lines are shown in Figure 4. As can be seen, the overlap factor  $\gamma$  increases with increasing generation, reaching 5.0 for the 4th and 5th generations. This last value is comparable with highly branched polymers.<sup>42</sup> The change of  $\gamma$  from low to high generation shows the change into different molecular character. Comparing the values of  $\gamma$  with  $k_H\phi_H/\phi = k$  from Table 3, we find that  $\gamma$  is between 20% and 30% smaller. The usefulness of the formula is restricted to  $0.2 < \phi < 0.4$ .

At the high-concentration range of the diffusion data, the limits of the NMR apparatus used were reached. Not every diffusion coefficient could be measured with the precision of the lower concentration ranges. The transversal and longitudinal relaxation times became very short. This made measurements for the 2nd, 3rd, and 4th generation very difficult especially at 5 °C. In Figure 3a the long time diffusion coefficients could therefore not be given above a certain concentration. Strangely enough, the relaxation times of the 1st and 5th generation were still large enough to measure diffusion coefficients. Relaxation times of magnetic spin moments can become shorter due to dipolar exchange between different hydrogen spins. Concentrating samples can facilitate this effect. Nevertheless, it is not clear why this should influence the 2nd to the 4th generation more than generations 1 and 5. The measurements of the 1st and 5th generations are as a consequence the most accurate.

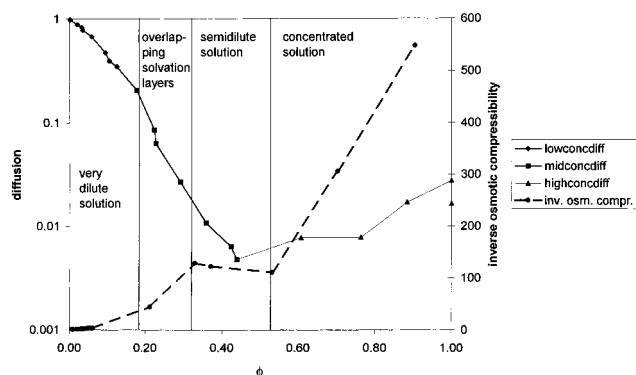


**Figure 5.** Comparison between the inverse osmotic compressibility and the diffusion data for the 5th generation at 25 °C.

## Discussion and Conclusions

The low volume fraction limit  $D_0$  of five generations of poly(propylene imine) dendrimers was determined for three different temperatures: 5, 25, and 45 °C. From this, radii  $R_H$  were determined that were found to be almost equal to the viscosity radii. Their behavior could be described by nondraining hard spheres, as the radius of gyration,  $R_G$ , is smaller than  $R_H$ . The viscosity mainly causes the temperature dependence of the diffusion coefficient. Only for the two highest generations was the radius effected by the temperature. For small volume fractions the first virial coefficient was measured. It was for most temperatures and generations found to be smaller than the hard sphere value with a radius  $R_H$ . The dendrimers thus behave like soft spheres. The exception is that at 5 °C the 4th and the 5th generation dendrimers behave like hard spheres. This is an indication for the lower quality of the solvent at low temperatures.

From the diffusion data it can be concluded that there exist different diffusion regimes: the very dilute, an intermediate regime, and, for the two highest generations, the concentrated regime. In the very dilute concentration regime,  $\phi < 0.20$ , the interactions between the dendrimers can be described using one virial coefficient (eq 2). This regime is characterized by the fact that the solvation layers do not overlap.

For higher volume fractions the single exponent is found to be inadequate for all but the lowest generation. The free volume formula was found to be more appropriate. Fits could be made for volume fractions,  $0.2 < \phi < 0.4$ . This is the part of the dilute regime where the solvation layers overlap,  $0.2 < \phi < 0.3$ , and includes part of the semidilute regime,  $0.3 < \phi < 0.4$ . In the concentrated regime for the 4th and 5th generation we were not able to obtain values converging with the long time self-diffusion coefficients.

It is interesting to compare the behavior of the diffusion data and the inverse osmotic compressibility as a function of the concentration.<sup>22</sup> This especially, because the diffusion data give dynamic information, whereas the equation of state is static. For the first generation, the equation of state could not be determined. The diffusion of these first generation dendrimers was characterized by the absence of different regimes. These molecules behave like normal, small molecules. The 2nd through the 5th generation show only a very gradual decrease through the dilute and semidilute regimes. The inverse osmotic compressibility has a very clear maximum at a volume fraction of about 0.3, where the system becomes semidilute. A similar

change in behavior for the diffusion coefficient is not found. It should be emphasized that the transition from dilute to semidilute behavior, found from the inverse osmotic compressibility, is not a sharp transition from the one thermodynamic phase to another.

The most notable change in behavior for the diffusion coefficients is a transition to free volume behavior when the solvation layer starts to overlap. The solvation layer is much more important for diffusion than for the osmotic compressibility, where the interaction radius is important. In Figure 5 the different regimes are shown. For the concentrated regime we could not obtain converging long time diffusion coefficients. In the figure the nonconverged values are given in this regime for comparison.

**Acknowledgment.** We thank J. Hollander for assistance with the measurements and valuable discussions. We thank J. de Bleijser for his fruitful discussions. We especially thank J. A. M. Smit for his support.

## References and Notes

- (1) Scherrenberg, R.; Coussens, B.; Van Vliet, P.; Edouard, G.; Brackman, J.; De Brabander, E. *Macromolecules* **1998**, *31*, 456–461.
- (2) Pötschke, D.; Ballauff, M.; Lindner, P.; Fischer, M.; Vögtle, F. *Macromolecules* **1999**, *32*, 4079–4087.
- (3) Uppuluri, S.; Keinath, S. E.; Tomalia, D. A.; Dvornic, P. R. *Macromolecules* **1998**, *31*, 4498–4510.
- (4) Mengerink, Y.; Mure, M.; De Brabander, E. M. M.; Vd. Wal, S. J. *J. Chromatogr. A* **1996**, *730*, 75–81.
- (5) Hummelen, J. C.; Van Dongen, J. L. J.; Meijer, E. W. *Chem. Eur. J.* **1997**, *3*, 1489–1493.
- (6) Murat, M.; Grest, G. S. *Macromolecules* **1996**, *29*, 1278–1285.
- (7) Cai, C.; Chen, Z. Y. *Macromolecules* **1998**, *31*, 6393–6396.
- (8) Balogh, L.; Tomalia, D. A. *J. Am. Chem. Soc.* **1998**, *120*, 7355–7356.
- (9) Boris, D.; Rubinstein, M. *Macromolecules* **1996**, *29*, 7251–7260.
- (10) Imae, T.; Funayama, K.; Aoi, K.; Tsutsumiuchi, K.; Okada, M.; Furusaka, M. *Langmuir* **1999**, *15*, 4076–4084.
- (11) Cavallo, L.; Fraternali, F. *Chem. Eur. J.* **1998**, *4*, 927–934.
- (12) Lescanec, R. L.; Muthukumar, M. *Macromolecules* **1990**, *23*, 2280–2288.
- (13) Mansfield, M. L.; Klushin, L. I. *Macromolecules* **1993**, *26*, 4262–4268.
- (14) Welch, P.; Muthukumar, M. *Macromolecules* **1998**, *31*, 5892–5897.
- (15) Topp, A.; Bauer, B. J.; Tomalia, D. A.; Amis, E. J. *Macromolecules* **1999**, *32*, 7232–7237.
- (16) Stechemesser, S.; Eimer, W. *Macromolecules* **1997**, *30*, 2204–2206.
- (17) Gorman, C. B.; Smith, J. C.; Hager, M. W.; Parkhurst, B. L.; Sierzputowska-Gracz, H.; Haney, C. A. *J. Am. Chem. Soc.* **1999**, *121*, 9958–9966.
- (18) Ihre, H.; Hult, A.; Söderlind, E. *J. Am. Chem. Soc.* **1996**, *118*, 6388–6395.
- (19) Newkome, G. R.; Young, J. K.; Baker, G. R.; Potter, R. L.; Audoly, L.; Cooper, D.; Weis, C. D.; Morris, K.; Johnson, C. S. *Macromolecules* **1993**, *26*, 2394–2396.
- (20) Young, J. K.; Baker, G. R.; Newkome, G. R.; Morris, K. F.; Johnson, C. S. *Macromolecules* **1994**, *27*, 3464–3471.
- (21) Hawker, C. J.; Farrington, P. J.; Mackay, M. E.; Wooley, K. L.; Frechet, J. M. J. *J. Am. Chem. Soc.* **1995**, *117*, 4409–4410.
- (22) Rietveld, I. B.; Bedeaux, D.; Smit, J. A. M., submitted for publication to *J. Colloid Interface Sci.*
- (23) Topp, A.; Bauer, B. J.; Prosa, T. J.; Scherrenberg, R.; Amis, E. J.; *Macromolecules* **1999**, *32*, 8923–8931.
- (24) Stilbs, P. *Prog. NMR Spectrosc.* **1987**, *19*, 1–45.
- (25) Stejskal, E. O. *J. Chem. Phys.* **1965**, *43*, 3597.
- (26) Tanner, J. E. *J. Chem. Phys.* **1970**, *52*, 2523.
- (27) Rietveld, I. B.; Smit, J. A. M. *Macromolecules* **1999**, *32*, 4608–4614.
- (28) Prosa, T. J.; Bauer, B. J.; Amis, E. J.; Tomalia, D. A.; Scherrenberg, R. *J. Polym. Sci., Part B: Polym. Phys.* **1997**, *35*, 2913–2924.
- (29) Murat, M.; Grest, G. S. *Macromolecules* **1996**, *29*, 1278–1285.

- (30) De Gennes, P. G.; Herve, H. J. *Phys. Lett. (Paris)* **1983**, *44*, 351–360.
- (31) Tomalia, D. A.; Naylor, A. M.; Goddard, W. A., III *Angew. Chem., Int. Ed. Engl.* **1990**, *29*, 138–175.
- (32) Fréchet, J. M. J. *Science* **1994**, *263*, 1710–1715.
- (33) Mourey, T. H.; Turner, S. R.; Rubinstein, M.; Fréchet, J. M. J.; Hawker, C. J.; Wooley K. L. *Macromolecules* **1992**, *25*, 2401–2406.
- (34) Cai, C.; Chen, Z. Y. *Macromolecules* **1997**, *30*, 5104–5117.
- (35) Dhont, J. K. G. *An Introduction to the Dynamics of Colloids*; Elsevier: Amsterdam, The Netherlands, 1996.
- (36) Batchelor, G. K. *J. Fluid Mech.* **1976**, *74*, 1–29.
- (37) Felderhof, B. U. *Physica A* **1977**, *89*, 373–384.
- (38) Elimelech, M.; Gregory, J.; Jia, X.; Williams, R. A. *Particle Deposition and Aggregation, Measurement, Modelling and Simulation*; Butterworth-Heinemann: Woburn, MA, 1995; pp 93–95.
- (39) Cohen, M. H.; Turnbull, D. *J. Chem. Phys.* **1959**, *31*, 1164.
- (40) Vrentas, J. S.; Duda, J. L.; Ling, H. C. *J. Polym. Sci., Polym. Phys.* **1985**, *23*, 275–288.
- (41) Vrentas, J. S.; Duda, J. L.; Ling, H. C. *J. Polym. Sci., Polym. Phys.* **1985**, *23*, 289–304.
- (42) Garver, T. M.; Callaghan, P. T. *Macromolecules* **1991**, *24*, 420–430.

MA000509E